Evaluation of anomalies during nickel and titanium silicide formation using the effective heat of formation model

R. Pretorius, C.C. Theron and T.K. Marais

Ion–Solid Interaction Division, Van de Graaff Group, National Accelerator Centre, Faure 7131 (South Africa)

H.A. Ras

Division of Microelectronics and Communications Technology, Council for Scientific and Industrial Research, Pretoria 0002 (South Africa)

Abstract

The effective heat of formation model allows heats of formation to be calculated as a function of the concentration of the reactants at the growth interface. The effective concentration is taken to be the concentration of the liquidus minimum for the relevant binary system. Using this model, the anomalous and contradictory results for initial formation of titanium silicide phases are ascribed to the two eutectics at 14 and 84 at.% silicon (both at 1330 °C) for the Ti–Si binary system. The native oxide layer usually present on silicon surfaces and the affinity of Ti for oxygen further affect the effective concentration, thereby adding to the contradictory experimental results that have been found. In the Ni–Si system our measurements show that a sufficiently high concentration of oxygen in amorphous silicon can lead to formation of NiSi instead of Ni_2Si, which is normally the first phase to form. This observation, as well as the formation of $NiSi_2$ as the first phase in the presence of diffusion barriers, is also explained in terms of the effective heat of formation model.

Introduction

The transition metal silicides have been studied extensively owing to their importance in gate metallization, as interconnects, and as ohmic and Schottky contacts in VLSI and ULSI devices [1, 2]. $TiSi_2$ in particular has been widely used, since it has a very low electrical resistivity of about 13 $\mu\Omega$ cm [2]. There has nevertheless been considerable uncertainty regarding initial phase formation at the interface between thin Ti films and single crystal silicon, with a wide variety of silicide phases such as $TiSi_2$, $TiSi$, Ti_5Si_4 and Ti_5Si_3 having been found [3–25]. It has also been stated that these contradictory results, as well as the observed sequence of growth of different silicide phases, are not in agreement with thermodynamic considerations [26]. In the case of the nickel silicides Ni_2Si is nearly always found to be the first phase to form [27, 28]. However, in the case of the reaction of nickel with amorphous silicon, certain authors have found NiSi to be the predominant first phase [28], while $NiSi_2$ is the first phase to form in structures where there is a diffusion barrier between the Ni metal layer and the single crystal silicon substrate [29]. In this investigation we have studied the interaction of thin Ni films with amorphous silicon in order to

determine how the oxygen content in the silicon affects phase formation. We also show how the anomalous behaviour of titanium and nickel silicide formation can be explained thermodynamically by using the 'effective heat of formation model' [30–34]. Thermodynamic [35] and crystallographic [36] data for the equilibrium Ni-silicide and Ti-silicide phases are given in Table 1.

Experimental

Thin Ni films ranging in thickness from about 100 to 400 nm were deposited onto Si⟨100⟩ and Si(a) substrates *in vacuo* with a 3 kW electron-gun system. The Si(a) substrates were obtained by evaporating silicon onto Si⟨100⟩ with an interposing Ni 'glue' layer of about 10 nm to promote better adhesion. The layer of amorphous silicon was always thicker than that necessary to transform all of the metal layer to the most silicon-rich phase. Oxygen was selectively introduced into the Si(a) layer by leaking oxygen gas into the evaporation chamber during deposition. By maintaining a constant oxygen pressure, relatively uniform doping throughout the Si(a) could be obtained. The pressure was regulated manually by controlling the gas flow with a needle

TABLE 1. Crystallographic and thermodynamic data for equilibrium Ni-silicide and Ti-silicide phases[a]

Phase	Congruency	Crystal system	Atoms per unit cell	ΔH^0 (kJ (mol at.)$^{-1}$)
Ni_3Si	NC	cubic	4	-37
Ni_5Si_2	C	hexagonal	43 or 14	-42
Ni_2Si	C	orthorhombic	12	-47
Ni_3Si_2	NC	orthorhombic	80	-45
$NiSi$	C	orthorhombic	8	-42
$NiSi_2$	NC	cubic	12	-29
Ti_3Si	NC	tetragonal	32	-53
Ti_5Si_3	C	hexagonal	16	-72
Ti_5Si_4	NC	tetragonal	36	-81
$TiSi$	NC	orthorhombic	8	-79
$TiSi_2$	C	orthorhombic	24	-57

[a]Crystallographic data from ref. 36; thermodynamic data from ref. 35.

valve, while at the same time pumping with the ion pump. Using progressively higher oxygen partial pressures, correspondingly higher levels of oxygen doping could be obtained. Evaporation was carried out at rates of about 0.5 nm s^{-1} and at pressures ranging from about 8×10^{-8} kPa, in the case of no intentional oxygen doping, to 9×10^{-6} kPa. Sample heating was carried out in a vacuum tube furnace at about 5×10^{-8} kPa. The silicide composition and growth was measured by Rutherford back-scattering (RBS) and X-ray diffraction. The detector angle was at 165° and a beam of 2 MeV alpha particles was used for the RBS measurements.

The effective heat of formation model

Because of the sustained interest in silicon–silicide interfaces for practical device applications in recent years, there is a need for a theoretical treatment of first phase formation and phase sequence in thin film diffusion couples [13]. The first attempts [37, 38] at formulating rules to predict first phase formation and phase formation sequence acknowledged the importance of metal–silicon equilibrium phase diagrams. The rule of Walser and Bené states that 'the first compound nucleated in planar binary reaction couples is the most stable congruently melting compound adjacent to the lowest temperature eutectic in the binary phase diagram' [37]. Although these rules were semiempirical, they emphasized the contribution that the lowest eutectic of the binary system made to phase selection. However, reports of metastable phase formation [3] in thin film growth led researchers to mistrust the use of equilibrium phase diagrams in predicting phase formation [39]. The influence of kinetic factors was highlighted and assumed to take precedence over equilibrium considerations [39, 40]. Attempts at formalizing phase growth in terms of

bulk equilibrium thermodynamics were dismissed [40, 41].

The effective heat of formation model combines both elements of equilibrium thermodynamics and kinetic considerations [30–34] and has successfully been applied to a large number of silicide [30, 31], aluminide [32, 33] and Au metal [34] thin-film couples. It has also been shown to explain results obtained by ion-beam mixing [42]. Predictions using the model are based on standard heats of formation, equilibrium phase diagrams and the incorporation of kinetic considerations through a dependence on the availability of atoms at the reaction interface. The availability of atoms is expressed as an effective concentration, and the effective heat of formation, $\Delta H'$, is defined as

$$\Delta H' = \Delta H^0 \times \frac{\text{effective conc. of limiting elem.}}{\text{compound conc. of limiting elem.}} \quad (1)$$

the standard heat of formation, ΔH^0, being expressed in joules per mole of atoms. The concept of a limiting element is closely connected to the effective concentration at which the formation of a specific compound phase is considered. At every reaction interface in binary systems the two elements will be available for reaction in a specific ratio (the effective concentration), and when forming a specific compound the elements will be consumed in the compound ratio. Whenever the effective concentration of a specific element is less than its compound concentration, that element is the limiting element. For instance, if the effective concentration is 40 at.% Si at the growth interface in the Ti–Si binary system, silicon would be the limiting element if the phase $TiSi_2$ ($Ti_{0.333}Si_{0.667}$) were to be formed. It is the limiting element and the effective concentration that are of importance and, when linked to the standard heat of formation through the effective heat of formation model, determine which compound phase is favoured thermodynamically for interfacial reaction. It should
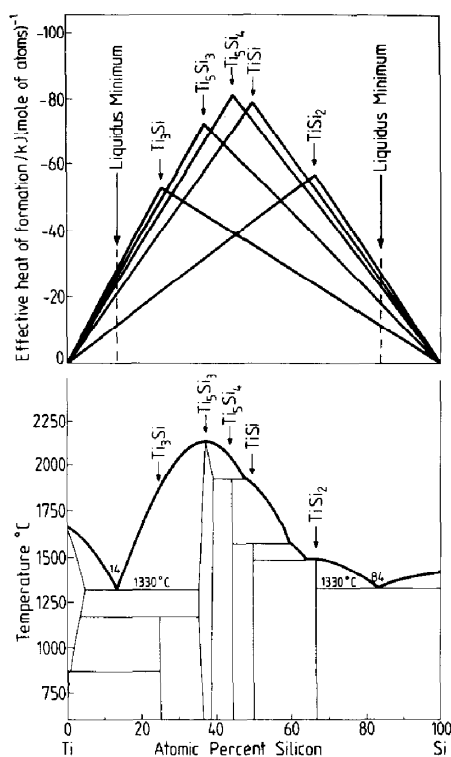
Fig. 1. The effective heat of formation ($\Delta H'$) diagram for compound formation (top) and phase diagram (bottom) for the Ti–Si system. Each triangle represents the energy released during the formation of a particular silicide phase, as a function of concentration. These diagrams are constructed by plotting the heats of formation (ΔH^0) for each compound at its composition and completing the triangulation by drawing a line to each end of the concentration axis.

be emphasized that the model predicts only the chemical composition and not whether the compound phase will be amorphous or metastable. Also, although the model may predict that formation of a certain phase will lead to the biggest free energy change, this phase may not form owing to nucleation problems at the moving reaction interface. This has proved to be the case for the Pt-aluminides [33], where certain phases have large numbers of atoms per unit cell.

Brown and Ashby [43] have shown that for a given structure and bond type, the activation energy for solid state diffusion is directly proportional to the melting point of the solid. The greatest mobility of the atoms and the most effective mixing at a reaction interface upon heating are therefore expected to take place at the composition of the liquidus minimum of the binary system. The effective concentration is therefore assumed to be that concentration leading to the highest mobility and is thus given by the composition at the liquidus minimum of the binary system [30–34].

Although the exclusion of noncongruent phases during silicide formation is not fully understood, it has been recognized that these phases do not nucleate easily

and are usually 'skipped' [37, 44]. The rule for predicting silicide formation therefore states that 'the first compound phase to form during metal–silicon interaction is the congruent phase with the most negative effective heat of formation ($\Delta H'$) at the concentration of the liquidus minimum of the binary system' [30, 31]. Note that the observation that noncongruent phases are 'skipped' does not preclude their possible formation in some systems from first principles. The effective heat of formation model also gives a quantitative reason for the large margin of success achieved by the semiempirical rules of Walser and Bené [37], since by considering eutectics, which for silicides invariably is the liquidus minimum [45], they had inadvertently taken the effect of concentration into consideration.

The effective heats of formation as a function of concentration for the various phases in a binary system can best be described graphically, as in Fig. 1 for the Ti–Si system. A certain amount of care should be exercised when evaluating these diagrams, since the exactness of the construction belies the uncertainties associated with the thermodynamic quantities. These values can have errors of up to 10% [46]. An arbitrary range of 5% has been suggested to interpret the data. From a purely thermodynamic point of view, therefore, there is not much to choose between phases with effective heats of formation within 5% of each other.

Titanium–silicon interaction

Many studies have been carried out regarding first phase formation during the reaction between thin Ti films and Si substrates. The $TiSi_2$ phase is reported to be the only phase found for temperatures greater than 500 °C [3–9]. In another study $TiSi_2$ was also reported as a first phase, but titanium-rich silicides were observed to grow on top of the disilicide layer [10]. Contrary to these reports, other studies show that all the titanium is converted to TiSi prior to formation of $TiSi_2$ at temperatures between 450 and 700 °C [9, 19, 20]. In low-temperature reactivity investigations a silicide corresponding to the monosilicide was also found together with unreacted but intermixed material [21], and transmission electron microscope (TEM) studies revealed nominal growth of TiSi at room temperature [14]. The formation of TiSi at temperatures of 450 °C [22] and 625 °C [23] is reported for rapid thermal annealing (RTA) as well. However, not all RTA studies show the initial formation of TiSi, as there is evidence for the first phase formation of Ti_5Si_4 after 6 s RTA at 600 °C [24]. In contrast to reports of the formation of an initial crystalline phase, the formation of an amorphous Ti–Si alloy before the appearance of any silicide is reported for temperatures not exceeding 450 °C [5], yet Lur and Chen [25], who also report on the formation

of an amorphous interlayer, always detect a diffraction ring corresponding to TiSi in all annealed samples.

The complexity of the Ti–Si system is reflected not only by the conflicting reports on identification of a first phase, but also by numerous reports of simultaneous phases that are found initially. A layered structure containing Ti_5Si_3, TiSi and $TiSi_2$ is reported for e-beam-deposited titanium [11], while Ti_5Si_3, Ti_5Si_4 and TiSi were found initially at intermediate temperatures between 400 and 600 °C [14]. On the other hand, the presence of Ti_5Si_3 and TiSi in sputter-deposited samples was reported [12, 13], yet quantitative Auger electron spectroscopy (AES) [15] showed the coexistence of Ti_5Si_3 and $TiSi_2$ for evaporated titanium, and these phases were also confirmed by RBS and TEM studies for RTA samples [16]. Furthermore, TEM and diffraction studies have shown the formation of $TiSi_2$ with traces of TiSi [17], while RBS and X-ray diffraction (XRD) also revealed these two phases for RTA [18].

It is well known that two polytypes of $TiSi_2$ exist, namely the equilibrium $TiSi_2$ having the C54 structure (face-centered orthorhombic lattice) and a phase having the C49 structure (base-centered orthorhombic lattice) [6], which is often referred to as a metastable phase [3]. These polytypes are well characterized by their resistivities, with the C49 phase having a resistivity of between 60 and 80 $\mu\Omega$ cm and the C54 phase having a resistivity of 13 $\mu\Omega$ cm [6]. Many investigations show the initial formation of C49 $TiSi_2$ [3–6] undergoing a transformation to C54 $TiSi_2$.

While annealing thin titanium on silicon at sufficiently high temperatures and sufficiently long times always leads to the formation of $TiSi_2$ eventually [14], the kinetics of the reaction is not so reproducible [9]. It was possible to show diffusion-limited growth, $t^{1/2}$ dependence, for the formation of $TiSi_2$ regardless of silicon substrate type [7–13]; however, Pico and Lagally [20] have shown in a direct investigation of phase thickness that the kinetics of $TiSi_2$ formation depends upon the orientation of the substrates, with $TiSi_2$ growing linearly with time on Si(111) and parabolically with time on Si(100). When the total silicide thickness is considered, a nearly parabolic growth rate on all substrates is reported [20].

All these conflicting and varying reports on first phase formation place considerable demands on any model attempting to explain the formation of an initial phase. The only phase given in the Ti–Si equilibrium phase diagram not reported to form initially is Ti_3Si. It is only when concentrations at a growth interface are taken into consideration that an understanding of the results can be attained. When applying the effective heat of formation model to the Ti–Si system, the most important variable is the effective concentration at the reaction interface. The most striking feature of the assessed equilibrium phase diagram (lower half of Fig. 1) of the Ti–Si system is the existence of two minima on the liquidus curve at the same temperature, 1330 °C. A Ti-rich eutectic exists at 14 at.% Si and a Si-rich eutectic is found at 84 at.% Si. According to the effective heat of formation model, the highest mobility of atomic mixing can occur at these two atomic ratios, and since these minima are at the same temperature a clear choice between the two cannot be made. The possibility naturally also exists that the true effective concentration lies somewhere between the two eutectics. The effect of eutectic concentrations close to each other in temperature on the effective concentration at the growth interface is not well understood and needs further study. In Table 2 the effective heats of formation for Ti–Si are calculated, assuming the effective concentration to be either at the concentration of the Si-rich liquidus minimum or the Ti-rich liquidus minimum. It is immediately apparent that an effective concentration of 84 at.% Si favours the formation of the silicon-rich silicide $TiSi_2$, with $\Delta H' = -27.4$ kJ (mol at.)$^{-1}$, while an effective concentration of 14 at.% Si favours the more titanium-rich silicides.

TABLE 2. Effective heats of formation $(\Delta H')^a$ for the titanium silicides

Phase	Compound concentration	ΔH^0	Effective concentrations			
			$Ti_{0.160}Si_{0.840}$		$Ti_{0.860}Si_{0.140}$	
			Limiting element	$\Delta H'$ (kJ (mol at.)$^{-1}$)	Limiting element	$\Delta H'$ (kJ (mol at.)$^{-1}$)
Ti_3Si	$Ti_{0.750}Si_{0.250}$	-53	Ti	-11.3	Si	$\underline{-29.7}$
Ti_5Si_3	$Ti_{0.625}Si_{0.375}$	-72	Ti	-18.4	Si	-26.9
Ti_5Si_4	$Ti_{0.556}Si_{0.444}$	-81	Ti	-23.3	Si	-25.5
TiSi	$Ti_{0.500}Si_{0.500}$	-79	Ti	-25.3	Si	-22.1
$TiSi_2$	$Ti_{0.333}Si_{0.667}$	-57	Ti	$\underline{-27.4}$	Si	-12.0

^{a}Calculated at the concentrations of the two lowest eutectics (both at 1330 °C) at 14 and 84 at.% silicon in the Ti–Si phase diagram. The predicted phases are those with the most negative $\Delta H'$ and are underlined.

Since the thermodynamics of the system is shown to be critically dependent on the effective concentration, impurities at the growth interface must play a major role in phase formation by determining the availability of atoms for reaction. This is not unreasonable, as it has been argued that the role impurities play at the interface strongly affects the reproducibility and the kinetics of phase formation [10]. Titanium has a well-known affinity for oxygen [13], and this tendency, coupled with the ever-present native oxide on the silicon substrate and the two eutectics at 1330 °C, is expected to lead to unpredictable effective concentrations at the interface. These effects will be more acute when deposition techniques such as sputtering are used, because impurities will differ in the sputtering ambients and these have been shown to be important in the determination of the first growing phase [9]. If, as proposed [13], the native oxide on the Si surface and the oxygen in the Ti act as diffusion barriers, the cleanliness of the surface will determine the availability of atoms at the reaction interface and could provide thermodynamic conditions favouring a number of different phases. The effective heat of formation model therefore predicts that the Ti–Si system should be highly influenced by impurities, and not surprisingly this is borne out by the mass of conflicting reports on first phase formation [3–25].

Nickel–silicon interaction

Thin nickel films react with silicon to form Ni_2Si as the first phase at temperatures as low as 200 °C [27, 28, 47, 48]. After all the nickel is consumed, the Ni_2Si reacts with the remaining silicon to form NiSi [47, 48] and at higher temperatures further reaction takes place to form $NiSi_2$ at about 750 °C for single crystal silicon [49] and 400 °C for amorphous silicon substrates [50]. This is the last phase to form for thin Ni on thick Si structures. The growth rate for first phase Ni_2Si is parabolic in time and is therefore diffusion limited [27, 28, 47, 48], with marker [51] and radioactive tracer [52] experiments showing that Ni is the dominant diffusing species.

Although Ni_2Si is normally the first phase to form in binary Ni–Si thin film structures, early work on the interaction between Ni and amorphous silicon formed by electron-beam evaporation showed that NiSi was predominantly the first phase [28]. Our RBS measurements (see top spectrum in Fig. 2) and X-ray diffraction measurements do, however, show that Ni_2Si is the first phase to form with amorphous silicon, similar to findings with single crystal silicon. As the oxygen content of the Si(a) layer is increased to about 8 at.% or higher, we find a reduced growth rate of Ni_2Si
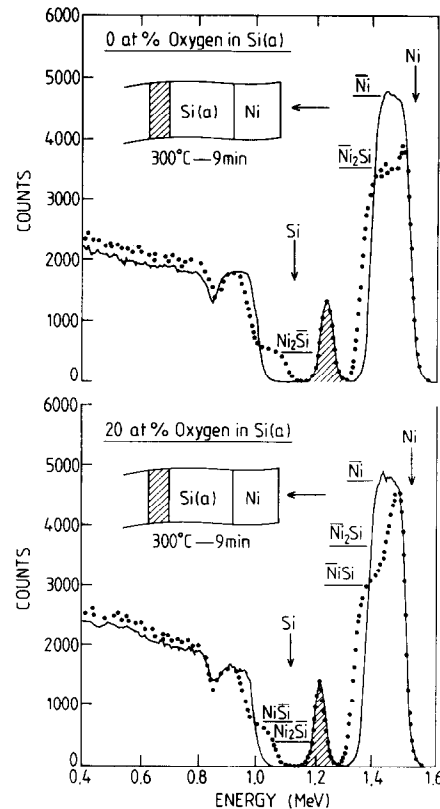

Fig. 2. Rutherford back-scattering spectra showing Ni_2Si first phase formation in a clean system (top) and NiSi formation for oxygen-contaminated amorphous silicon (bottom). The cross-hatched peak is the nickel 'glue' layer, which ensures good adhesion of the Si(a) layer to the Si⟨100⟩ substrate.

accompanied by the simultaneous growth of NiSi, while at an oxygen concentration of about 20 at.% it can be seen (see bottom spectrum in Fig. 2) that NiSi instead of Ni_2Si is the first phase to form. We therefore suspect that in the early study [28] of nickel interaction with Si(a), first phase formation of both Ni_2Si and NiSi can be ascribed to the presence of relatively large concentrations of oxygen in the Si(a) layer. Silicon is known to be a getter of oxygen, and at pressures of 8×10^{-7} kPa, oxygen concentrations greater than 10 at.% have been found in amorphous silicon layers formed by evaporation [53]. The other low-temperature (966 °C) eutectic, at 56 at.% Si for the Ni–Si system (see Fig. 3, bottom), will further affect the effective concentration in such a way as to favour NiSi formation. Other workers, studying Pt-encapsulated $Ni_{80}Cr_{20}$ thin films on single crystal silicon heated at temperatures ranging from 300 to 500 °C, also find first phase NiSi formation [54]. It was observed that the Cr atoms segregate at the original Si|NiCr interface to form an amorphous layer, while Ni diffused through this Cr-rich amorphous layer, which acts as a permeable membrane selectively passing Ni to form a very uniform NiSi layer. During a study of Si⟨111⟩|NiZr|Ni structures [29], it was found
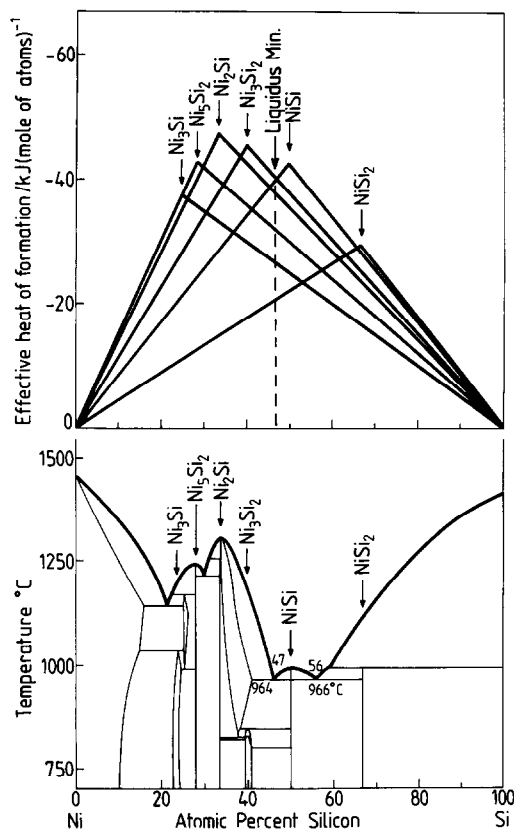
Fig. 3. The effective heat of formation diagram and phase diagram for the Ni–Si system. At the concentration of the liquidus minimum, formation of the Ni_3Si_2 phase will lead to the largest free energy change, but because noncongruent phases are skipped, formation of Ni_2Si or NiSi is favoured, depending on the experimental conditions. In the presence of diffusion barriers the effective concentration of Ni can be reduced and that of Si increased into a region (greater than 66 at.% Si) that favours $NiSi_2$ first phase formation.

that at temperatures as low as 350 °C, Ni diffuses through the amorphous NiZr barrier layer leading to the formation of epitaxial $NiSi_2$. This result is regarded as very surprising, as $NiSi_2$ is usually the last phase to form with thick single crystal silicon at temperatures greater than 750 °C [49].

We thus see that Ni_2Si, NiSi or $NiSi_2$ can be the first phase to form, depending on experimental conditions. This rather anomalous behaviour of nickel silicide formation is summarized schematically in Fig. 4. To understand these experimental observations let us look at the effective heat of formation diagram for the Ni–Si binary system, given in Fig. 3. It can be seen that at the concentration of the lowest eutectic (47 at.% Si), formation of Ni_3Si_2 will lead to the biggest free energy change. This is, however, a noncongruent phase which in the case of silicides is difficult to nucleate and is usually skipped [2, 37]. This leaves the two congruent phases Ni_2Si and NiSi, which have effective heats of formation of -36.6 and -39.5 kJ (mol at.)$^{-1}$,
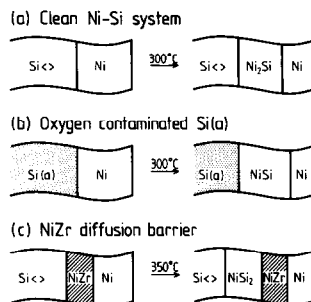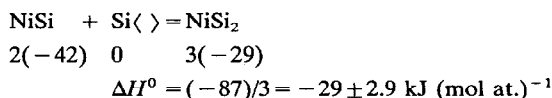

Fig. 4. Schematic illustration showing that Ni_2Si, NiSi or $NiSi_2$ can be the first phase to form, depending on experimental conditions which affect the effective concentration at the growth interface, thereby thermodynamically favouring the formation of a particular phase.
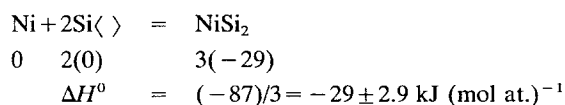
respectively, at an effective concentration of 47 at.% silicon. If one considers that thermodynamic data can easily have errors of up to 10%, it is clear that from a thermodynamic point of view there is not much to choose between the formation of Ni_2Si and NiSi. Although entropy changes are very small during solid state interaction [46] and can usually be ignored, this is not the case when the effective heats of formation are very close to each other, as in cases such as this. Also, if the silicon is doped with oxygen to levels above about 8 at.% oxygen, as was the case in this study, the effective concentration of Si relative to that of Ni apparently increases to above about 45 at.% Si, at which concentration formation of NiSi is thermodynamically favoured (see Fig. 3). In the case of Si⟨ ⟩|NiZr|Ni structures, the NiZr apparently acts as a diffusion barrier and further reduces the effective concentration of nickel relative to that of silicon, so that $NiSi_2$ forms as the first phase at the Si⟨ ⟩|NiZr interface [54]. This means that the relative effective concentration of silicon at the reaction interface must be greater than about 66 at.% Si, which is in a region where $NiSi_2$ formation is thermodynamically favoured (see Fig. 3).

The normal temperature for $NiSi_2$ formation with single crystal silicon [49] is above 750 °C, and it therefore seems strange that $NiSi_2$ can form at temperatures as low as 370 °C in the presence of a NiZr diffusion barrier [29]. This anomalous behaviour can, however, be explained thermodynamically. In the case of normal $NiSi_2$ formation, NiSi reacts with single crystal silicon to form $NiSi_2$, whereas in Si⟨ ⟩|NiZr|Ni structures [29], $NiSi_2$ forms directly as the first phase. The heats of reaction for these two cases can be calculated from the ΔH^0 values in Table 1.

(a) Normal $NiSi_2$ formation (Si⟨ ⟩|Ni):

$$NiSi + Si\langle \rangle = NiSi_2$$
$$2(-42) \quad 0 \qquad 3(-29)$$
$$\Delta H^0 = (-87)/3 = -29 \pm 2.9 \text{ kJ (mol at.)}^{-1}$$

(b) $NiSi_2$ formation with barrier $(Si\langle\ \rangle|NiZr|Ni)$:

$$Ni + 2Si\langle\ \rangle\ =\ NiSi_2$$
$$0\quad 2(0)\qquad\quad 3(-29)$$
$$\Delta H^0\ =\ (-87)/3 = -29\pm2.9\ kJ\ (mol\ at.)^{-1}$$

It can thus be seen that the heat of reaction for $NiSi_2$ formation without a barrier is for all practical purposes zero (taking a 10% error into account), and it is only at higher temperatures that the entropy term $T\Delta S$ makes the free energy negative. In the case of $NiSi_2$ first phase formation in $Si\langle\ \rangle|NiZr|Ni$ structures, the heat of reaction is very negative and a high temperature is not needed to make the reaction thermodynamically possible.

Conclusions

We have used the effective heat of formation model [30–34] to explain the anomalous phase formation observed during titanium silicide formation. The model makes it possible to calculate heats of formation as a function of the relative concentration of the reactants at the growth interface. As phase formation during solid state interaction is a dynamic, nonequilibrium process, the effective concentration differs from the true physical concentrations at the growth interface. Although many factors could influence the effective concentration, the overriding factor apparently is the lowest point on the liquidus curve of the binary phase diagram, as greater mobility of atoms is expected at such a concentration [43]. The effective concentration at the growth interface is therefore taken to be that of the composition at the liquidus minimum. The anomalous phase formation behaviour of the titanium silicides is ascribed to the fact that the Ti–Si binary system has two eutectic minima on the liquidus curve, at 14 and 84 at.% Si, both at a temperature of 1330 °C. The true effective concentration can therefore be anywhere between these two values, and the effective heat of formation model thus predicts a whole range of phases, as is found experimentally. Because of this, the Ti–Si system is very sensitive to impurities such as oxygen, which can further influence the effective concentration.

During nickel–silicon interaction Ni_2Si is the first phase to form with single crystal silicon and amorphous silicon in clean systems [27, 28, 47, 48]. Our measurements do, however, show that for oxygen concentrations in the amorphous silicon above about 8 at.%, both Ni_2Si and NiSi form initially, with the amount of NiSi increasing with oxygen content, until it is the only phase to form at oxygen concentrations greater than 20 at.%. At the composition of the liquidus minimum for the Ni–Si binary system there is thermodynamically not much to choose between the formation of Ni_2Si

and NiSi. The presence of oxygen in the amorphous silicon does apparently increase the effective concentration of Si into a region where the effective heat of formation diagram shows that NiSi formation is thermodynamically favoured. In $Si\langle\ \rangle|NiZr|Ni$ structures [29] the NiZr layer acts as a diffusion barrier, thereby further reducing the effective concentration of nickel and increasing that of silicon to a concentration region where $NiSi_2$ formation will lead to the biggest free energy change.

To summarize, phase formation depends on the thermodynamics of the system, as well as the concentration of the reacting species at the growth interface. The effective heat of formation model links thermodynamics and concentration (and therefore kinetics) by defining an effective heat of formation which is concentration dependent. By using this model we are able to explain the anomalous behaviour observed during formation of titanium and nickel silicides.

References

1 S.P. Murarka, *Silicides for VLSI Applications*, Academic Press, New York, 1983.
2 M.-A. Nicolet and S.S. Lau, in N. Einspruch (ed.), *VLSI Electronics: Microstructural Science*, Academic Press, New York, 1983, p. 329.
3 R. Beyers and R. Sinclair, *J. Appl. Phys., 57* (1985) 5240.
4 W.K. Chu, S.S. Lau, J.W. Mayer, H. Muller and K.N. Tu, *Thin Solid Films, 25* (1975) 393.
5 I.J.M.M. Raaijmakers, A.H. Reader and P.H. Oosting, *J. Appl. Phys., 63* (1988) 2790.
6 J.C. Hensel, J.M. Vandenberg, F.C. Unterwald and A. Maury, *Appl. Phys. Lett., 51* (1987) 1100.
7 R.W. Bower and J.W. Mayer, *Appl. Phys. Lett., 20* (1972) 359.
8 A. Guldan, V. Schiller, A. Steffan and P. Balk, *Thin Solid Films, 100* (1983) 1.
9 L.S. Hung, J. Gyulai, J.W. Mayer, S.S. Lau and M.-A. Nicolet, *J. Appl. Phys., 54* (1983) 5076.
10 G.G. Bentini, R. Nipoti, A. Armigliato, M. Berti, A.V. Drigo and C. Cohen, *J. Appl. Phys., 57* (1985) 270.
11 J.S. Maa, C.J. Lin and J.H. Lin, *Thin Solid Films, 64* (1979) 439.
12 H. Kato and Y. Nakamura, *Thin Solid Films, 34* (1976) 135.
13 C.C. Hsu, Y.X. Wang, S.D. Yin, B.Q. Li, M.R. Ji and J.X. Wu, *J. Vac. Sci. Technol. A, 5* (1987) 1402.
14 S.T. Lakshmikumar and A.C. Rastogi, *J. Vac. Sci. Technol. B, 7* (1989) 604.
15 C. Queniset, R. Naslain and P. Demoney, *Surf. Interface Anal., 13* (1988) 123.

38

16 K. Shenai, P.A. Piacente, N. Lewis, G.a. Smith, M.D. McConnell and B.J. Baliga, *J. Vac. Sci. Technol. B*, 6 (1988) 1728.

17 R. Butz, G.W. Rubloff, T.Y. Tan and P.S. Ho, *Phys. Rev. B*, 30 (1984) 5421.

18 D. Levy, J.P. Ponpon, A. Grob, J.J. Grob and R. Stuck, *Appl. Phys. A*, 38 (1985) 23.

19 S.P. Murarka and D.B. Fraser, *J. Appl. Phys.*, 51 (1980) 342.

20 C.A. Pico and M.G. Lagally, *J. Appl. Phys.*, 64 (1988) 4957.

21 G.W. Rubloff, R.M. Tromp and E.J. van Loenen, *Appl. Phys. Lett.*, 48 (1986) 1600.

22 R.J. Nemanich, R.T. Fulks, B.L. Stafford and H.A. Vander Plas, *J. Vac. Sci. Technol. A*, 3 (1985) 938.

23 C.S. Wei, J. Van der Spiegel and J. Santiago, *J. Vac. Sci. Technol. A*, 3 (1985) 2259.

24 C.X. Dexin, H.B. Harrison and G.K. Reeves, *J. Appl. Phys.*, 63 (1988) 2171,

25 W. Lur and L.J. Chen, *Appl. Phys. Lett.*, 54 (1989) 1217.

26 M.A. Taubenblatt and C.R. Helms, *J. Appl. Phys.*, 53 (1982) 6308.

27 K.N. Tu, W.K. Chu and J.W. Mayer, *Thin Solid Films*, 25 (1975) 403.

28 J.O. Olowolafe, M.-A. Nicolet and J.W. Mayer, *Thin Solid Films*, 38 (1976) 143.

29 R. de Reus, H.C. Tissink and F.W. Saris, *J. Mater. Res.*, 5 (1990) 341.

30 R. Pretorius, *Mater. Res. Soc. Symp. Proc.*, 25 (1984) 15.

31 R. Pretorius, *Vacuum*, 41 (1990) 1038.

32 R. Pretorius, R. de Reus, A.M. Vredenberg and F.W. Saris, *Mater. Lett.*, 9 (1990) 494.

33 R. Pretorius, R. de Reus, A.M. Vredenberg and F.W. Saris, *J. Appl. Phys.*, 70 (1991) 3636.

34 R. Pretorius, T.K. Marais, A.E. Muller and D. Knoesen, *Mater. Res. Soc. Symp. Proc.*, 238 (1992) 475.

35 M.E. Schlesinger, *Chem. Rev.*, 90 (1990) 607.

36 P. Villars and L.D. Calvert, *Pearson's Handbook of Crystallographic Data for Intermetallic Phases*, Vol. 3, American Society for Metals, Metal Park, OH, 1989.

37 R.M. Walser and R.W. Bené, *Appl. Phys. Lett.*, 28 (1976) 624.

38 B.Y. Tsaur, S.S. Lau, J.W. Mayer and M.-A. Nicolet, *Appl. Phys. Lett.*, 38 (1981) 922.

39 U. Gösele and K.N. Tu, *J. Appl. Phys.*, 53 (1982) 3252.

40 R.W. Bené, *J. Appl. Phys.*, 61 (1987) 1826.

41 E.G. Colgan, *J. Appl. Phys.*, 62 (1987) 1224.

42 W. Xia, M. Fernandes, C.A. Hewett, S.S. Lau, D.B. Poker and J.P. Biersack, *Nucl. Instr. Methods*, 37 (1989) 408.

43 A.M. Brown and M.F. Ashby, *Acta Metall.*, 24 (1980) 1088.

44 E.G. Colgan, B.Y. Tsaur and J.W. Mayer, *Appl. Phys. Lett.*, 37 (1981) 511.

45 T.B. Massalski, *Binary Alloy Phase Diagrams*, American Society for Metals, Metal Park, OH, 1986.

46 O. Kubaschewski and C.B. Alcock, *Metallurgical Thermochemistry*, Pergamon, Oxford, 1979, p. 268.

47 D.M. Scott and M.-A. Nicolet, *Nucl. Instr. Methods*, 182 (1981) 655.

48 D.J. Coe and E.H. Rhoderick, *J. Phys. D*, 9 (1976) 965.

49 F. D'Heurle, S. Petersson, L. Stolt and B. Stritzker, *J. Appl. Phys.*, 53 (1982) 5678.

50 C.D. Lien, M.-A. Nicolet and S.S. Lau, *Appl. Phys. A*, 34 (1984) 249.

51 W.K. Chu, H. Krautle, J.W. Mayer, H. Muller, M.-A. Nicolet and K.N. Tu, *Appl. Phys. Lett.*, 25 (1974) 454.

52 R. Pretorius, C.L. Ramiller, S.S. Lau and M.-A. Nicolet, *Appl. Phys. Lett.*, 30 (1977) 501.

53 H.A. Ras, The Solid State Chemistry of Co–Si and Ni–Si Binary Thin Film Systems, *Ph.D. Thesis*, University of Stellenbosch, South Africa, 1987.

54 G.E. Rozgonyi, J.H. Lee, D. Knoesen, D. Adams, B. Patnaik, N. Parikh, A.S.M. Salih and P. Balducci, *Appl. Phys. Lett.*, 58 (1991) 729.